Lamin aggregation is an early sensor of porphyria-induced liver injury

Amika Singla[1], Nicholas W. Griggs[1], Raymond Kwan[1], Natasha T. Snider[1], Dhiman Maitra[1], Stephen A. Ernst[2], Harald Herrmann[4] and M. Bishr Omary[1,3,*]

[1]Department of Molecular and Integrative Physiology, University of Michigan Medical School, Ann Arbor, MI 48109, USA
[2]Department of Cell and Developmental Biology, University of Michigan Medical School, Ann Arbor, MI 48109, USA
[3]Department of Medicine, University of Michigan Medical School, Ann Arbor, MI 48109, USA
[4]Functional Architecture of the Cell Group, German Cancer Research Center, 69120 Heidelberg, Germany
*Author for correspondence (mbishr@umich.edu)

Accepted 9 April 2013
Journal of Cell Science 126, 3105–3112

doi: 10.1242/jcs.123026

Summary

Oxidative liver injury during steatohepatitis results in aggregation and transglutaminase-2 (TG2)-mediated crosslinking of the keratin cytoplasmic intermediate filament proteins (IFs) to form Mallory-Denk body (MDB) inclusions. The effect of liver injury on lamin nuclear IFs is unknown, though lamin mutations in several human diseases result in lamin disorganization and nuclear shape changes. We tested the hypothesis that lamins undergo aggregation during oxidative liver injury using two MDB mouse models: (i) mice fed the porphyrinogenic drug 3,5-diethoxycarbonyl-1,4-dihydrocollidine (DDC) and (ii) mice that harbor a mutation in ferrochelatase (fch), which converts protoporphyrin IX to heme. Dramatic aggregation of lamin A/C and B1 was noted in the livers of both models in association with changes in lamin organization and nuclear shape, as determined by immunostaining and electron microscopy. The lamin aggregates sequester other nuclear proteins including transcription factors and ribosomal and nuclear pore components into high molecular weight complexes, as determined by mass-spectrometry and confirmed biochemically. Lamin aggregate formation is rapid and precedes keratin aggregation in fch livers, and is seen in liver explants of patients with alcoholic cirrhosis. Exposure of cultured cells to DDC, protoporphyrin IX or *N*-methyl-protoporphyrin, or incubation of purified lamins with protoporphyrin IX, also results in lamin aggregation. In contrast, lamin aggregation is ameliorated by TG2 inhibition. Therefore, lamin aggregation is an early sensor of porphyria-associated liver injury and might serve to buffer oxidative stress. The nuclear shape and lamin defects associated with porphyria phenocopy the changes seen in laminopathies and could result in transcriptional alterations due to sequestration of nuclear proteins.

Key words: Lamin aggregation, Liver injury, Porphyria, Mallory-Denk bodies

Introduction

Intermediate filament proteins (IFs), microtubules and microfilaments, form the major components of the cytoskeleton (Ku et al., 1999). IFs are widely expressed in a cell- and tissue-dependent manner and are divided into 6 types based on similarities in their protein structure (Fuchs and Cleveland, 1998; Goldman et al., 2008; Herrmann et al., 2009). Types I–IV are cytoplasmic IFs, including keratins, vimentin and neurofilaments; type V represent the nuclear lamins; and type VI include the lens-specific proteins Bfsp1 and Bfsp2 (Fuchs and Cleveland, 1998; Goldman et al., 2008; Herrmann et al., 2009). Structurally, IFs consist of a central α-helical 'rod' domain that is flanked by non-α-helical N-terminal 'head' and C-terminal 'tail' domains (Fuchs and Cleveland, 1998; Ku et al., 1999; Goldman et al., 2008; Herrmann et al., 2009).

The nuclear lamin IFs represent the major component of the nuclear lamina, and are found beneath the inner nuclear membrane and form part of the nuclear envelope (Dechat et al., 2008; Worman, 2012). Lamins play important roles in providing structural integrity, DNA replication, protein trafficking and gene transcription (Dechat et al., 2008; Worman, 2012). They are classified into A- and B-types, with A-type lamins being found mainly in differentiated cells, whereas B-type lamins being expressed in all cells throughout development (Dechat et al., 2008; Worman, 2012). A-type lamins include lamins A and C, which are derived from a single *LMNA* gene by alternative splicing. Lamin A and C differ in their carboxy terminus, with lamin A containing a CaaX motif. B-type lamins include lamin B1 and B2 proteins that are derived from the *LMNB1* and *LMNB2* genes respectively (Dechat et al., 2008; Worman, 2012).

IFs are involved in various human diseases that are tissue selective (Fuchs and Cleveland, 1998; Omary et al., 2004). Mutations in lamin genes lead to variety of laminopathies including muscular dystrophies, lipodystrophy, cardiomyopathies and premature aging (Dechat et al., 2008; Bertrand et al., 2011; Worman, 2012). IFs are also involved in the formation of protein inclusions independent of IF mutation (Omary et al., 2004; Omary, 2009). For example, the cytoplasmic IFs, keratins 8 and 18 (K8/K18), undergo aggregation and formation of inclusions called Mallory-Denk bodies (MDBs) which are commonly seen in several forms of liver injury particularly those related to alcoholic and non-alcoholic steatohepatitis (Zatloukal et al., 2007). MDBs are induced in mice by feeding the porphyrinogenic compound 3,5-diethoxycarbonyl-1,4-dihydrocollidine (DDC) for 3 months (Zatloukal et al., 2007). MDB formation requires several cellular events including crosslinking of keratins by transglutaminase-2

(TG2) and site-specific keratin phosphorylation (Omary et al., 2009; Strnad and Omary, 2009; Kwan et al., 2012). Lamins are also known to undergo aggregation in various laminopathies, such as in Hutchinson-Gilford progeria syndrome (Dechat et al., 2008), and become oxidized via conserved C-terminal cysteine residues in response to cell senescence (Pekovic et al., 2011). However, the effect of oxidative liver injury on lamins, and whether lamins aggregate independent of lamin mutation are unknown.

Given the importance of lamins in several critical nuclear functions, and the fact that keratins and lamins belong to the same IF class family, we hypothesized that lamins also undergo aggregation during liver injury in a manner that is similar to keratins. We tested this hypothesis in both drug-induced and genetically-linked porphyria models. Our findings demonstrate the formation of lamin aggregates in both of these models. Importantly, we show that lamin aggregation is an early event as compared to keratin aggregation, and is likely to be related to direct cross-linking by porphyrin and possibly via transamidation by TG2.

Results

Formation of lamin aggregates in drug- and genetic-induced porphyria models

We examined the changes in lamin proteins in livers of C57BL mice fed DDC for 3 months. Notably, there was a decrease in the lamin B1 and A/C monomers with concurrent formation of lamin high molecular weight (MW) complexes exclusively in the livers from the DDC-fed animals (Fig. 1A). To determine if the lamin aggregation is drug-specific or if it can be similarly observed in a genetic model of spontaneous MDB formation that is also associated with porphyria (Singla et al., 2012), we isolated the nuclear fractions from the Fech^{m1Pas} mice [which harbor a mutation in the ferrochelatase (fch) gene] (Tutois et al., 1991). We found prominent formation of lamin high MW complexes in homozygous (fch/fch) mice as compared to wild-type (wt/wt) and heterozygous (wt/fch) mice (Fig. 1A). Furthermore, immunofluorescence staining for lamin B1 showed the presence of lamin aggregates and misshapen nuclei in fch/fch versus wt/wt mice (Fig. 1B). Lamin A/C and lamin B1 aggregate formation was also observed in DDC-fed mice as determined by immunofluorescence staining (supplementary material Fig. S1). Presence of misshapen nuclei in conjunction with nuclear membrane lobulations and loss of the peripheral heterochromatin was also confirmed by electron microscopy of fch/fch livers (Fig. 1C). Nuclear staining of liver tissue sections confirmed the nuclear shape changes in fch livers (Fig. 1D), with percent of cells with round nuclei being 71±2% in wild-type livers and 28±2% in fch livers.

To further characterize the composition of nuclear aggregates, we analyzed the high MW protein bands visualized by Coomassie staining in the fch/fch but not control livers (Fig. 2A) using mass spectrometry. Peptides corresponding to

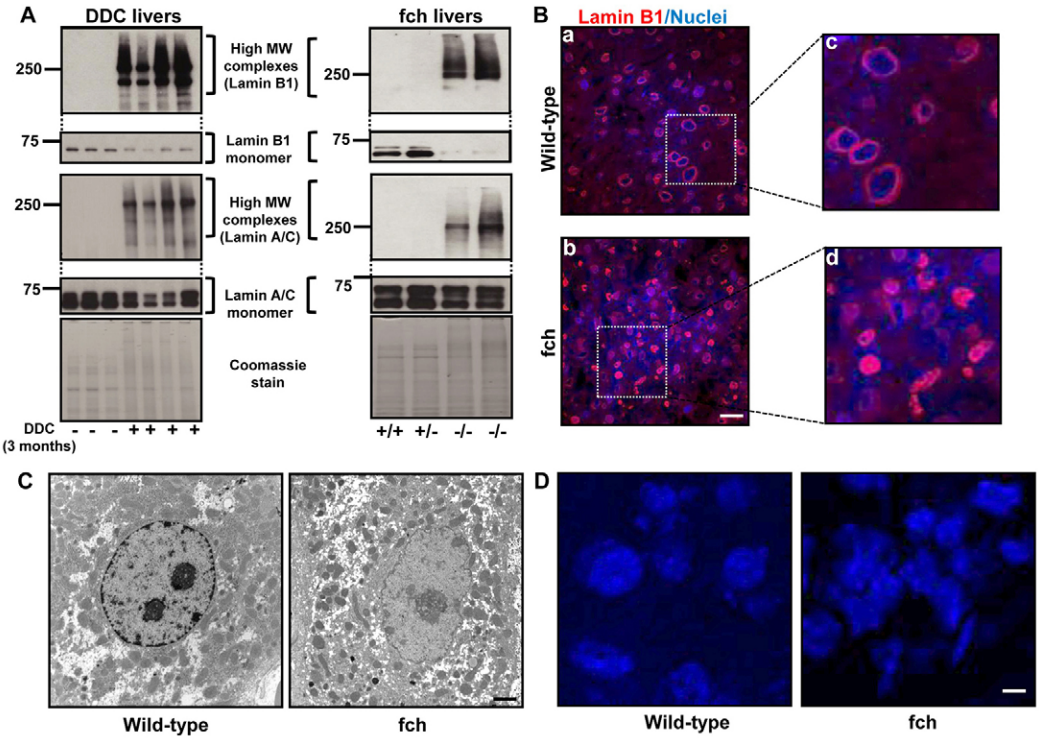

Fig. 1. Lamin aggregates are present in DDC-fed and fch/fch mice. (**A**) Liver nuclear extracts were prepared from C57BL mice (controls or DDC-fed for 3 months) or from 5-month-old wt/wt (+/+), wt/fch (+/−) and fch/fch (−/−) mice, then subjected to 8% SDS-PAGE and immunoblotted with antibodies to lamin B1 and A/C. Two images with different exposure times are shown for each gel. The lower panel for each gel represents the shorter exposure (10 seconds) and shows the lamin monomer, whereas the upper panels show the longer exposure image (10–30 minutes) and depict the lamin high MW complexes. Coomassie stain of the nuclear extracts is included to show equal protein loading. (**B**) Immunofluorescence staining was performed on liver sections from wild-type and fch/fch mice. Lamin B1 is shown in red and nuclei are shown in blue. Panels Bc and Bd show higher magnification of the boxed areas in Ba and Bb, respectively. (**C**) Transmission electron microscopy was carried out on livers from wild-type and fch/fch mice. (**D**) Liver sections from wild-type and fch/fch mice were stained with DAPI to determine nuclear shape. Scale bars: 5 μm.

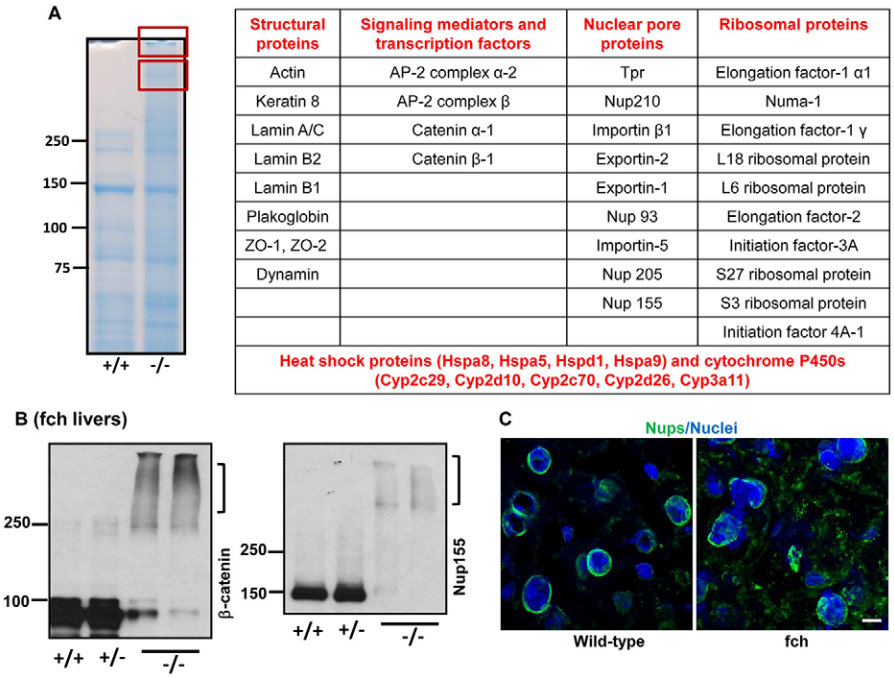

Structural proteins	Signaling mediators and transcription factors	Nuclear pore proteins	Ribosomal proteins
Actin	AP-2 complex α-2	Tpr	Elongation factor-1 α1
Keratin 8	AP-2 complex β	Nup210	Numa-1
Lamin A/C	Catenin α-1	Importin β1	Elongation factor-1 γ
Lamin B2	Catenin β-1	Exportin-2	L18 ribosomal protein
Lamin B1		Exportin-1	L6 ribosomal protein
Plakoglobin		Nup 93	Elongation factor-2
ZO-1, ZO-2		Importin-5	Initiation factor-3A
Dynamin		Nup 205	S27 ribosomal protein
		Nup 155	S3 ribosomal protein
			Initiation factor 4A-1
Heat shock proteins (Hspa8, Hspa5, Hspd1, Hspa9) and cytochrome P450s (Cyp2c29, Cyp2d10, Cyp2c70, Cyp2d26, Cyp3a11)			

Fig. 2. Mass spectrometry analysis and validation of high MW complexes isolated from fch/fch mice. (**A**) Nuclear extracts from wild-type (+/+) and fch/fch (−/−) liver were subjected to 8% SDS-PAGE followed by staining of the gel with Coomassie Blue. Extracts from the fch/fch mice showed the presence of high MW bands (shown in the two red boxes). The boxed bands were excised and analyzed by mass spectrometry. The proteins that were identified by mass spectrometry were categorized as structural proteins, signaling mediators and transcription factors, nuclear pore proteins and ribosomal proteins. (**B**) Nuclear extracts from livers of wild-type, wt/fch (+/−) and fch/fch mice were analyzed by immunoblotting using antibodies to Nup155 and β-catenin. Brackets highlight the high MW species. (**C**) Liver sections from wild-type and fch/fch mice were stained for Nup proteins (green) and nuclei (blue) using mAb414 antibody. Scale bar: 5 µm.

numerous proteins were identified and categorized into structural proteins, signaling mediators, transcription factors, nuclear pore proteins (Nups) and ribosomal proteins (Fig. 2A). Aggregation (or potentially crosslinking) of some of the identified proteins (β-catenin, Nup155 and dynamin), with concurrent decrease in detection of the monomer, was validated by immune blotting (Fig. 2B and supplementary material Fig. S2A). Immunofluorescence staining, using antibody mAb414, showed mislocalization and aggregation of Nups in the liver of fch mice (Fig. 2C).

Lamin aggregation is an early event in response to liver injury

We then asked whether the changes in lamins is a late or early event in response to injury and how that compared with cytoplasmic protein changes that are known to involve keratins. Even short-term DDC-feeding (2 days) of C57BL mice is accompanied by formation of high MW lamins (Fig. 3A), while K8 showed the formation of lower molecular weight complexes and with lower relative intensity of antibody reactivity (Fig. 3B). Since DDC feeding is known to result in protoporphyrin IX (PPIX) accumulation via its inhibition of ferrochelatase (Zatloukal et al., 2007), we measured PPIX levels in the livers of DDC-fed mice after 2 days of feeding. PPIX levels were not detectable in controls, while PPIX levels after 2 days of DDC feeding were 248±8.7 pmol/mg of liver tissue. Additionally, immunofluorescence staining showed the presence of lamin aggregates and misshapen nuclei after 2 days DDC feeding (Fig. 3C). However, there were no obvious keratin aggregates or filament reorganization after 2 days of DDC feeding. These results suggest that lamin aggregation is an early event as compared with the cytoplasmic keratins. Furthermore, livers of mice fed griseofulvin for 5 days, which also causes porphyria and liver injury (Zatloukal et al., 2007), also results in the formation of prominent lamin high MW complexes (supplementary material Fig. S2B). The lamin aggregates that form in the liver after the short-term 2 days of DDC feeding are highly insoluble as evidenced by their increased presence in the pellet fraction as compared to the nuclear extract fraction (supplementary material Fig. S2C).

Given that MDB formation in fch/fch mice occurs progressively as the mice age (Singla et al., 2012), we examined the time course of lamin aggregation relative to keratin aggregation. Notably, fch/fch (−/−) livers accumulates lamin-containing high MW complexes as early as 1 month of age, at a time when keratin aggregates are not detectable (Fig. 3D). As shown in Fig. 3D, young fch mice showed marked formation of lamin but much less evidence of keratin high MW complexes. Taken together, lamin aggregation occurs rapidly in the context of porphyria that is associated with drug feeding (within 2 days) or in the genetic fch model (within 1 month), at a stage when changes in the cytoplasmic keratins are still modest.

Lamin aggregation occurs *in vitro* but is independent of direct oxidative injury

We then developed an *in vitro* cell culture lamin aggregation model utilizing human hepatoma HepG2 cells. Exposure of HepG2 cells to different doses of *N*-methyl protoporphyrin (NMP; the metabolite of DDC responsible for ferochelatase inhibition) for 48 hours resulted in a dose dependent decrease in lamin monomers with parallel increase in lamin high MW complex formation (Fig. 4A). Treatment of HepG2 cells with PPIX led to the formation of lamin high MW complexes in the nuclear fraction as early as 5 minutes after exposure (Fig. 4B). There was a dramatic loss of lamin monomers after 4 hours and 20 hours of PPIX exposure with reciprocal increases in lamin aggregates in the pellet fractions (Fig. 4B). Similarly primary mouse hepatocyte cultures treated with DDC also showed the changes in nuclear shape and a change in the lamin staining from the typical nuclear rim to the formation of puncta (Fig. 4C). Furthermore, to examine if the PPIX-mediated lamin aggregation is oxidation-related, HepG2 cells were pre-treated with *N*-acetyl cysteine (NAC) and incubated with

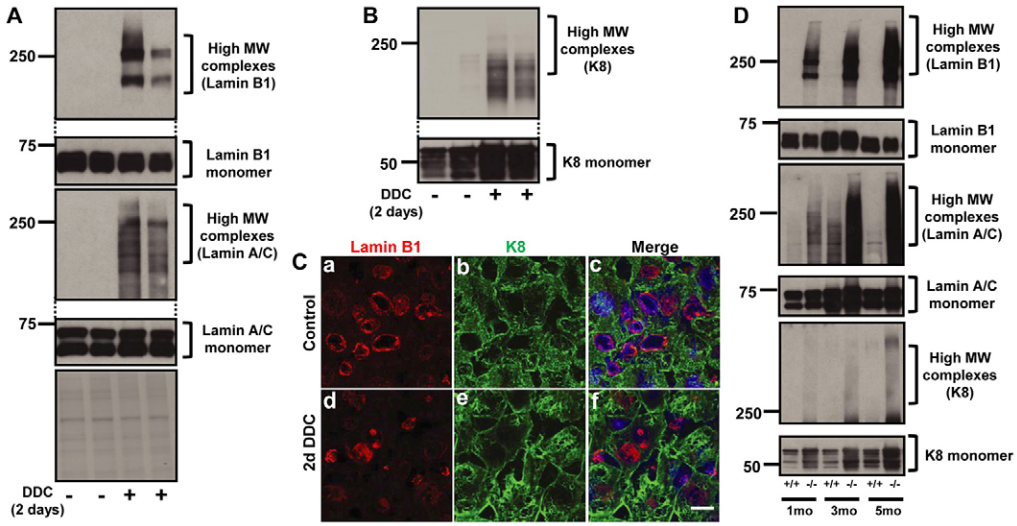

Fig. 3. Lamin aggregation in response to injury is a rapid event as compared with keratin aggregation. (**A**) C57BL mice were fed DDC for 2 days. Liver nuclear extracts were prepared and immunoblotted using antibodies to lamin B1 and A/C. The exposure of the upper and lower parts of the gel is similar to that shown in Fig. 1A,B. (**B**) HSE were prepared from controls and mice fed DDC for 2 days to obtain the relatively insoluble keratin-enriched fraction, followed by analysis by immunoblotting using anti-K8 antibody. (**C**) Liver sections from controls and mice fed DDC for 2 days were stained for lamin B1 (red) and K8 (green). Merged images also show the staining of nuclei (blue). (**D**) Nuclear extracts (lamins) and HSE (K8) from 1, 3 and 5-month-old wild-type and fch/fch animals were used to examine lamin B1, lamin A/C and K8 expression and aggregation. Scale bar: 5 μm.

different concentration of PPIX. As shown in supplementary material Fig. S3A, pre-treatment with NAC did not prevent the formation of lamin aggregates which suggests a direct PPIX effect.

Lamin aggregation is mediated by TG2 and via direct crosslinking by protoporphyrin IX

Since keratin aggregation during MDB formation requires crosslinking by TG2 (Strnad et al., 2007), we hypothesized that

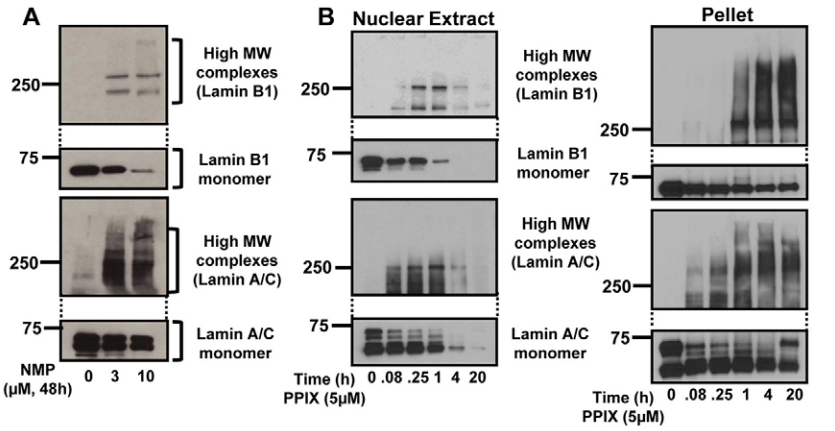

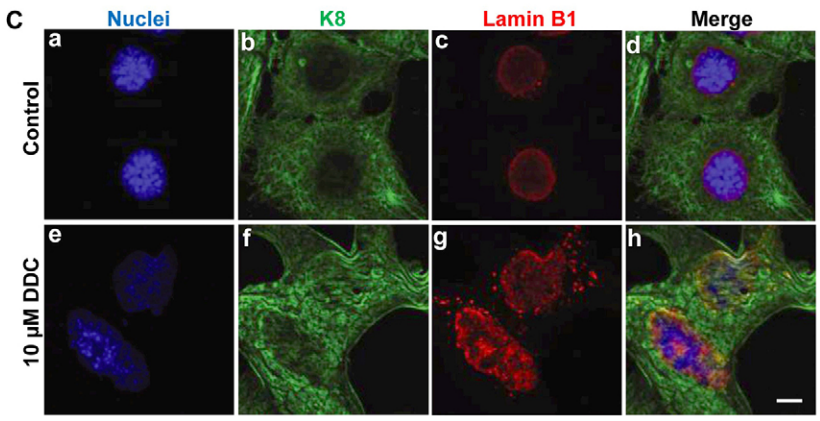

Fig. 4. Lamin aggregation occurs *in vitro*. (**A**) HepG2 cells were treated with vehicle, 3 or 10 μm of NMP for 48 hours. Nuclear extracts were prepared to assess lamin B1 and A/C aggregation. (**B**) HepG2 cells were treated with 5 μM PPIX for the indicated times followed by analysis of the nuclear extract or post-nuclear-extract pellet fraction by blotting using antibodies to lamins. (**C**) Hepatocytes were isolated from C57BL mice then treated with vehicle (control) or 10 μM DDC for 24 hours. Cells were then stained to image nuclei (blue), K8 (green) or lamins (red). Scale bar: 5 μm.

lamin aggregation might be related to transamidation by TG2. To test this hypothesis, we examined the transglutaminase (TG) activity in HepG2 cells after PPIX treatment as measured by incorporation of the TG small molecule substrate 5-(biotinamido)pentylamine (5-BP) into cellular proteins. As shown in Fig. 5A, incorporation of 5-BP into liver proteins was significantly enhanced upon treatment with PPIX. The increased incorporation of 5-BP was almost completely abolished in the presence of the TG2 inhibitor cystamine (Fig. 5B). Therefore, PPIX results in TG activation.

We then tested the effect of cystamine on lamin aggregation in cultured cells. Exposure of HepG2 cells to PPIX, with or without cystamine, results in the formation of high MW lamin species that decrease in the presence of cystamine (Fig. 5C). In addition, treatment of nuclear extracts from HepG2 cells or from normal mouse liver with recombinant TG2 resulted in lamin aggregation (Fig. 5D). Lamin aggregation was also investigated in TG2 overexpressing cells with or without PPIX treatment. As shown in supplementary material Fig. S3B, transfection of TG2 in the presence of PPIX results in a further decrease in the lamin B1 and A/C monomers as compared to PPIX-treated cells that are not transfected with TG2 (compare lanes 2 and 4). However, there was no change in the formation of lamin high MW complexes, which may be due to antibody epitope masking of what we predict are highly crosslinked high MW species. Collectively, these data suggest that PPIX-mediated lamin aggregation is related to crosslinking by TG.

Metalloporphyrins are known to mediate crosslinking of the proteins in the presence of oxidants (Campbell et al., 1998). Therefore, we tested whether lamin crosslinking can take place directly by PPIX. Incubation of purified lamins (lamin A and C) with PPIX resulted in lamin A and C crosslinking (Fig. 5E,F). Therefore, lamin crosslinking in the setting of porphyria, may take place directly by protoporphyrin in a non-enzymatic manner.

Lamin aggregates are also present in human end-stage liver disease samples

We compared the presence of lamin aggregates in liver explants from patients with alcoholic cirrhosis versus control normal human livers. Lamin-containing high MW species were noted only in cirrhotic livers (Fig. 6A). These results provide a potential clinical relevance of our findings.

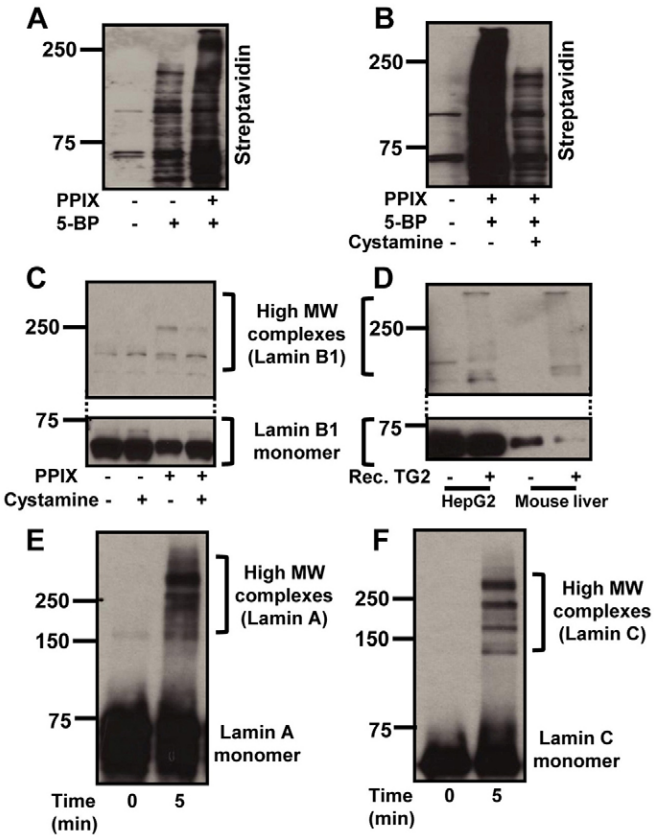

Fig. 5. Lamin aggregation is mediated in part by TG2 and by PPIX. (**A**) HepG2 cells were treated with 5 μM PPIX for 24 hours followed by incubating the cells with 1 mM 5-BP for 2 hours. Nuclear extracts were then prepared and blotted using streptavidin-HRP to examine 5-BP incorporation to cellular proteins. (**B**) HepG2 cells were pretreated with cystamine dihydrochloride for 1 hour followed by co-incubation with PPIX for 24 hours in the presence or absence of 5-BP for the last 2 hours. Nuclear extracts were then prepared and analyzed as for A. (**C**) Nuclear extracts were prepared from the cells with or without co-incubation with cystamine and PPIX, followed by blotting with anti-lamin B1 antibody. (**D**) Nuclear extracts from control HepG2 cells and from normal C57/BL mouse liver were incubated with 3.5 μg/ml of recombinant TG2 for 15 minutes. Nuclear extracts were then blotted using anti-lamin B1 antibody. (**E**,**F**) Purified lamins A (E) and C (F) were incubated with 5 μM PPIX for 5 minutes followed by the SDS-PAGE and blotting using anti-lamin A/C antibody.

Discussion

Lamin-containing aggregates form in the context of liver injury

Cytoplasmic IF proteins are known to exhibit aberrant organization and formation of IF aggregates in the form of inclusions as described for K8/K18 in alcoholic and non-alcoholic steatohepatitis (Zatloukal et al., 2007; Omary et al., 2009), glial fibrillary acidic protein in Alexander disease (Liem and Messing, 2009), and desmin in desmin-related myopathy (Sugawara et al., 2000). Similarly, the presence of nuclear lamin or cytoplasmic keratin aggregates (not inclusions per se, presumably due to the smaller-sized aggregates as compared to inclusions seen by standard hematoxylin and eosin staining) has been reported in several laminopathies (Dechat et al., 2008; Bertrand et al., 2011; Worman, 2012) and in the setting of epidermal keratin mutation in the Dowling-Meara form of epidermolysis bullosa simplex (Coulombe et al., 1991). Our findings demonstrate for the first time the presence of nuclear lamin aggregates in the absence of lamin mutation but in response to porphyria-mediated liver injury, which also reflects an oxidative form of liver injury (Hanada et al., 2010; Snider et al., 2011). Our findings are not able to distinguish whether lamin aggregation takes place en-route to the nucleus or directly in the nucleus. However, lamin aggregates are observed very rapidly (within 5 minutes) in the nuclear fraction (Fig. 4B).

Lamins are known to interact with several proteins and are involved in multiple cellular functions including maintenance of nuclear integrity, transcriptional regulation, signal transduction, DNA repair mechanisms and cell cycle control (Dechat et al., 2008; Andrés and González, 2009; Wilson and Foisner, 2010; Bertrand et al., 2011; Worman, 2012). Mislocalization and aggregation of lamins has been shown to perturb various cellular functions. For example, transfection of HeLa cells with mutant

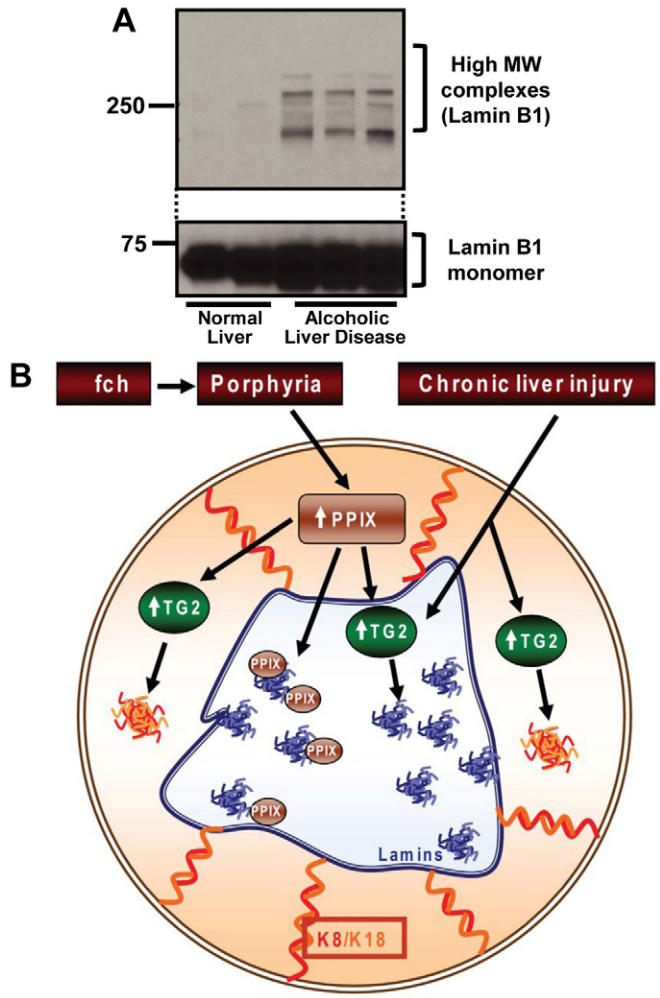

Fig. 6. Presence of lamin aggregates in liver explants of patients with alcoholic cirrhosis, and model of porphyria-mediated protein alterations. (**A**) Nuclei-enriched fractions from normal and alcoholic cirrhosis explant livers were analyzed by SDS-PAGE followed by blotting using anti-lamin B1 antibody. (**B**) Schematic model of lamin and keratin aggregate formation in response to porphyria or chronic liver injury. DDC or griseofulvin administration to mice, or a point mutation in fch, results in inactivation of ferrochelatase, thereby leading to the accumulation of PPIX. Accumulated PPIX activates TG2, which in the cytoplasm leads to formation of MDBs and in the nucleus can lead to formation of lamin aggregates. PPIX itself can further directly aggregate or crosslink lamins in the nucleus. The relative contribution of direct PPIX-mediated aggregation and TG2-mediated crosslinking are likely to be context dependent.

lamin A induced re-distribution of retinoblastoma protein and the sterol responsive element binding protein 1a into nuclear aggregates (Hübner et al., 2006). Similar to this but in the absence of lamin mutation, we identified various proteins as components of the high MW lamin-containing species including Nup155, β-catenin and dynamin. Nup155 is a nuclear pore complex protein, which along with other Nup proteins, importins and exportins plays a major role in nuclear trafficking (Kodiha et al., 2008). The presence of Nup155 in the aggregates we observed is consistent with the study showing the mislocalization and nuclear retention of nuclear transport proteins (Nup153, Nup88) in response to oxidative stress (Kodiha et al., 2008).

The major hallmark of naturally-occurring lamin mutations includes changes in nuclear shape and function (Dechat et al., 2008; Bertrand et al., 2011; Worman, 2012). The ultrastructural and immune staining analysis herein demonstrated the presence of irregular nuclei in fch/fch mice, which we attribute to porphyria and oxidative stress-related changes in lamins. These nuclear morphological changes are similar to what has been described in patients with lamin mutations (Dechat et al., 2008). In contrast and with respect to keratin aggregation, our findings indicated that lamin aggregation is an early event in porphyrogenic liver injury models and is noted in mice as early as 2 days after DDC feeding or in young fch/fch mice that do not harbor keratin aggregates. Hence, lamin aggregation appears to be a highly sensitive marker of porphyria-related injury.

The formation of lamin aggregates was also noted in liver explants from patients with alcoholic cirrhosis which provides a human clinical context to our findings. In this case, formation of such aggregates may be due to the activation of TG2 given that ethanol administration to mice results in TG2 activation and translocation to the nucleus coupled with crosslinking of Sp1 (Tatsukawa et al., 2009). Also, porphyria is not a feature of alcohol-related liver injury so a direct PPIX-mediated crosslinking or aggregation could not be invoked. Therefore, lamin aggregation is likely to take place in a variety of disease settings, but the extent and mode of aggregation is predictably context dependent.

Mechanisms involved in lamin aggregate formation

Our results showed a decrease in lamin monomers with formation of high MW lamin-containing complexes that we term aggregates due to their insolubility and stability to the presence of reducing agents. These aggregates were noted in livers from DDC-fed, griseofulvin-fed, and fch/fch mice. The decrease in the lamin monomer is consistent with another report that described loss of anti-lamin antibody reactivity to liver extracts isolated from griseofulvin-fed mice (Zatloukal et al., 1992). Several lines of evidence support the increase in oxidative load in the presence of porphyria. For example, the porphyria that is induced by DDC feeding or in the context of Fch mutation is associated with enhanced protein oxidation as measured biochemically (Hanada et al., 2010; Singla et al., 2012), altered bioenergetics with decreased liver ATP levels (Singla et al., 2012), and increased levels of hepatocyte reactive oxygen species (ROS) (Snider et al., 2011). In addition, PPIX increases intracellular H_2O_2 levels as noted in cultured HepG2 cells (Koningsberger et al., 1995). Therefore, the presence of lamin aggregates in drug and genetic-induced liver injury models is likely related to the oxidative stress caused by accumulated PPIX. These findings are consistent with recent observations showing that oxidant exposure to lamin A thiols, as occurs during exposure to ROS or during cell senescence, results in lamin oxidation at conserved cysteines (Pekovic et al., 2011). Conversely, patients with *LMNA* mutations exhibit increased sensitivity to oxidative stress and show elevated ROS levels (Malhas et al., 2009; Pekovic et al., 2011; Richards et al., 2011; Sieprath et al., 2012). Lamin B1 also plays a role in oxidative stress; for example, lamin B1 expression decreases under conditions of chronic oxidative stress and this decrease alters the anti-oxidant protein expression through regulation of p53 or Oct-1 (Malhas et al., 2009).

Although an increase in the oxidative load might trigger lamin aggregation, the downstream mediators of the aggregation are

likely to be multi-factorial and context dependent, and may not be related to direct oxidative injury per se (for example the oxidative scavenger NAC did not decrease lamin aggregate formation in HepG2 cells, supplementary material Fig. S3B). In the case of porphyria-associated liver injury, our findings indicate that two mediators of lamin aggregation are likely to be direct crosslinking by PPIX and possible involvement of TG2 in liver injury that involves TG2 activation but not porphyria (e.g. alcoholic liver disease). There was an increase in the activity and expression level of TG2 in fch mice, but TG2 itself is not found in the aggregates (either by the mass spectrometry analysis or by immune blotting, not shown). Any involvement of TG in lamin crosslinking is likely to be similar to its involvement in keratin transamidation and crosslinking (Strnad et al., 2007; Omary et al., 2009). Consistent with this, various stimuli are known to activate TG2 that is then involved in the crosslinking and modification of various nuclear proteins including histones, hypoxia inducible factor 1, Sp1 and E2F1 (Kuo et al., 2011). Another mechanism of lamin aggregation is direct modification by PPIX. The precise nature of modification by PPIX remains to be defined, including determining whether it involves crosslinking via bityrosines adducts (Campbell et al., 1998), though modification of histidines with or without crosslinking with consequent aggregation are also possible (Dubbelman et al., 1978). In addition, PPIX has been reported to inhibit cytochrome P450 enzymatic activity (Williams et al., 1992), although the exact nature of PPIX-cytochrome P450 adduct formation to our knowledge is not known. Taken together, our findings suggest a model (Fig. 6B) whereby accumulation of PPIX either activates both nuclear and cytoplasmic TG2 or it binds to nuclear proteins directly, thereby resulting in cytoplasmic and nuclear aggregate formation. Alternatively, TG2 may be activated via other insults to cause lamin aggregation. Direct characterization of PPIX adducts or transamidated peptides will be needed to help define the modified sites and proteins, and to clarify the specific mechanisms that are involved.

Materials and Methods

Reagents, tissues and animal experiments

The antibodies used included: K8 (Troma-I) (Developmental Studies Hybridoma Bank); lamin B1 and mAb414 (Abcam), and lamin A/C (Santa Cruz Biotechnology). All animal and human studies were approved by the Animal Use and Care Committee, and Human Subject Committee at the University of Michigan. C57BL animals were obtained from Jackson laboratories and were fed 0.1% DDC or 1.25% griseofulvin (Sigma-Aldrich) in LabDiet 5001 (PMI Nutrition International). Age and gender matched control mice were fed a standard mouse diet. $Fech^{m1Pas}$ mice (Balb/c background) were also obtained from Jackson Laboratories and were described previously (Singla et al., 2012). Mice were euthanized by CO_2 inhalation and livers were harvested and snap-frozen. Normal human livers were obtained from National Disease Research Interchange and the alcoholic cirrhosis livers explants were obtained without identifiers from patients with end-stage liver disease who underwent liver transplantation.

Nuclear extracts, high salt extracts and immunoblotting

Nuclear extracts were prepared using the NE-PER cytoplasmic/nuclear fractionation kit (Thermo Fisher Scientific). High salt extracts (HSE) were prepared as previously described to obtain keratin-enriched fractions (Ku et al., 2004). Equal protein amounts were loaded on 8% or 10% SDS-polyacrylamide gels and stained by Coomassie Blue or transferred to polyvinylidene-difluoride membranes and immunoblotted using relevant antibodies. High MW protein bands identified after Coomassie staining were excised from the gel and were analyzed using mass spectrometry after in-gel digestion of the gel strip with trypsin (MS Bioworks).

Hepatocyte isolation

Livers from C57BL mice were resected followed by hepatocyte isolation as described (Snider et al., 2011). Briefly, livers were perfused with Hank's balanced salt solution containing 0.5 mM EGTA, 5.5 mM glucose and 1% penicillin-streptomycin after the mouse was anesthetized with 50 mg/kg Nembutal (Lundbeck Inc.). Livers were then perfused with a solution containing Hanks balanced salt solution with 1.5 mM $CaCl_2$, 5.5 mM glucose, 1% penicillin-streptomycin and 2000 units of collagenase IV (Worthington Biochemical Corporation). Cells were then filtered using a 70-μm cell strainer and were cultured in William's medium E on collagen-coated dishes and were allowed to attach for 8 hours before treatment with DDC.

Immunofluorescence staining and electron microscopy

Liver sections and primary hepatocytes were fixed in acetone and methanol respectively, air-dried and stained as described (Ku et al., 2004; Snider et al., 2011). Stained tissues or cells were mounted with ProLong Gold containing DAPI (Invitrogen) and imaged using confocal microscopy (Fluoview 500; Olympus). For electron microscopy, 2-mm wide pieces of liver from wt/wt and fch/fch mice were fixed for 2 hours in phosphate buffered saline (PBS) containing 2% formaldehyde (prepared from paraformaldehyde) and 2% glutaraldehyde, and were then rinsed in PBS. Specimen were then post-fixed for 45 minutes with 1% aqueous OsO_4. Tissues were then dehydrated and embedded in Epon, stained with uranyl acetate and lead citrate, followed by image acquisition using a Philips CM-100 electron microscope.

Cell culture, transglutaminase experiments and lamin *in vitro* crosslinking

HepG2 human hepatoma cells (American Type Culture Collection) were cultured as recommended by the supplier. Cells were treated with *N*-methyl protoporphyrin (NMP) for 48 hours or with PPIX for different time points, followed by analysis by immunoblotting. For the detection of TG activity, control or treated cells were incubated with 1 mM 5-BP for 2 hours, followed by preparation of nuclear extracts then immunoblotting. Cell transfection with cDNA for TG2 was carried out using Lipofectamine 2000 (Invitrogen) in six-well plates (3–4 μg of DNA/well). After 48 hours, cells were harvested and nuclear extracts were prepared. Lamin crosslinking was carried out by incubating 500 nM of protein and 5 μM of PPIX for 5 minutes (22℃, 15 μl total volume). The reaction was quenched by adding equal volumes of 2× reducing Laemmli sample buffer, and samples were boiled for 5 minutes then analyzed after separation using 8% SDS-polyacrylamide gels.

Acknowledgements

We thank Dr Sujith V Weerasinghe for providing the mouse hepatocytes and Bradley Nelson for assistance with the electron microscopy.

Author contributions

A.S. and M.B.O. designed most of the experiments and wrote the manuscript. A.S. performed most of the experiments with assistance from N.W.G., R.K., N.T.S. and D.M. Essential reagents and technical expertise were provided by S.A.E. and H.H. All authors read and edited the manuscript.

Funding

This work was supported by the National Institutes of Health [grant number DK52951 to M.B.O., grant number DK34933 to the University of Michigan, grant number DK093202 to A.S., and grant number DK093776 to N.T.S.]; and by a Department of Veterans Affairs Merit Award to M.B.O. Deposited in PMC for release after 12 months.

Supplementary material available online at
http://jcs.biologists.org/lookup/suppl/doi:10.1242/jcs.123026/-/DC1

References

Andrés, V. and González, J. M. (2009). Role of A-type lamins in signaling, transcription, and chromatin organization. *J. Cell Biol.* **187**, 945-957.

Bertrand, A. T., Chikhaoui, K., Yaou, R. B. and Bonne, G. (2011). Clinical and genetic heterogeneity in laminopathies. *Biochem. Soc. Trans.* **39**, 1687-1692.

Campbell, L. A., Kodadek, T. and Brown, K. C. (1998). Protein cross-linking mediated by metalloporphyrins. *Bioorg. Med. Chem.* **6**, 1301-1307.

Coulombe, P. A., Hutton, M. E., Letai, A., Hebert, A., Paller, A. S. and Fuchs, E. (1991). Point mutations in human keratin 14 genes of epidermolysis bullosa simplex patients: genetic and functional analyses. *Cell* **66**, 1301-1311.

Dechat, T., Pfleghaar, K., Sengupta, K., Shimi, T., Shumaker, D. K., Solimando, L. and Goldman, R. D. (2008). Nuclear lamins: major factors in the structural organization and function of the nucleus and chromatin. *Genes Dev.* **22**, 832-853.

Dubbelman, T. M., de Goeij, A. F. and van Steveninck, J. (1978). Photodynamic effects of protoporphyrin on human erythrocytes. Nature of the cross-linking of membrane proteins. *Biochim. Biophys. Acta* **511**, 141-151.

Fuchs, E. and Cleveland, D. W. (1998). A structural scaffolding of intermediate filaments in health and disease. *Science* **279**, 514-519.

Goldman, R. D., Grin, B., Mendez, M. G. and Kuczmarski, E. R. (2008). Intermediate filaments: versatile building blocks of cell structure. *Curr. Opin. Cell Biol.* **20**, 28-34.

Hanada, S., Snider, N. T., Brunt, E. M., Hollenberg, P. F. and Omary, M. B. (2010). Gender dimorphic formation of mouse Mallory-Denk bodies and the role of xenobiotic metabolism and oxidative stress. *Gastroenterology* **138**, 1607-1617.

Herrmann, H., Strelkov, S. V., Burkhard, P. and Aebi, U. (2009). Intermediate filaments: primary determinants of cell architecture and plasticity. *J. Clin. Invest.* **119**, 1772-1783.

Hübner, S., Eam, J. E., Hübner, A. and Jans, D. A. (2006). Laminopathy-inducing lamin A mutants can induce redistribution of lamin binding proteins into nuclear aggregates. *Exp. Cell Res.* **312**, 171-183.

Kodiha, M., Tran, D., Qian, C., Morogan, A., Presley, J. F., Brown, C. M. and Stochaj, U. (2008). Oxidative stress mislocalizes and retains transport factor importin-alpha and nucleoporins Nup153 and Nup88 in nuclei where they generate high molecular mass complexes. *Biochim. Biophys. Acta* **1783**, 405-418.

Koningsberger, J. C., Rademakers, L. H., van Hattum, J., de la Faille, H. B., Wiegman, L. J., Italiaander, E., van Berge Henegouwen, G. P. and Marx, J. J. (1995). Exogenous protoporphyrin inhibits Hep G2 cell proliferation, increases the intracellular hydrogen peroxide concentration and causes ultrastructural alterations. *J. Hepatol.* **22**, 57-65.

Ku, N. O., Zhou, X., Toivola, D. M. and Omary, M. B. (1999). The cytoskeleton of digestive epithelia in health and disease. *Am. J. Physiol.* **277**, G1108-G1137.

Ku, N. O., Toivola, D. M., Zhou, Q., Tao, G. Z., Zhong, B. and Omary, M. B. (2004). Studying simple epithelial keratins in cells and tissues. *Methods Cell Biol.* **78**, 489-517.

Kuo, T. F., Tatsukawa, H. and Kojima, S. (2011). New insights into the functions and localization of nuclear transglutaminase 2. *FEBS J.* **278**, 4756-4767.

Kwan, R., Hanada, S., Harada, M., Strnad, P., Li, D. H. and Omary, M. B. (2012). Keratin 8 phosphorylation regulates its transamidation and hepatocyte Mallory-Denk body formation. *FASEB J.* **26**, 2318-2326.

Liem, R. K. and Messing, A. (2009). Dysfunctions of neuronal and glial intermediate filaments in disease. *J. Clin. Invest.* **119**, 1814-1824.

Malhas, A. N., Lee, C. F. and Vaux, D. J. (2009). Lamin B1 controls oxidative stress responses via Oct-1. *J. Cell Biol.* **184**, 45-55.

Omary, M. B. (2009). "IF-pathies": a broad spectrum of intermediate filament-associated diseases. *J. Clin. Invest.* **119**, 1756-1762.

Omary, M. B., Coulombe, P. A. and McLean, W. H. (2004). Intermediate filament proteins and their associated diseases. *N. Engl. J. Med.* **351**, 2087-2100.

Omary, M. B., Ku, N. O., Strnad, P. and Hanada, S. (2009). Toward unraveling the complexity of simple epithelial keratins in human disease. *J. Clin. Invest.* **119**, 1794-1805.

Pekovic, V., Gibbs-Seymour, I., Markiewicz, E., Alzoghaibi, F., Benham, A. M., Edwards, R., Wenhert, M., von Zglinicki, T. and Hutchison, C. J. (2011). Conserved cysteine residues in the mammalian lamin A tail are essential for cellular responses to ROS generation. *Aging Cell* **10**, 1067-1079.

Richards, S. A., Muter, J., Ritchie, P., Lattanzi, G. and Hutchison, C. J. (2011). The accumulation of un-repairable DNA damage in laminopathy progeria fibroblasts is caused by ROS generation and is prevented by treatment with N-acetyl cysteine. *Hum. Mol. Genet.* **20**, 3997-4004.

Sieprath, T., Darwiche, R. and De Vos, W. H. (2012). Lamins as mediators of oxidative stress. *Biochem. Biophys. Res. Commun.* **421**, 635-639.

Singla, A., Moons, D. S., Snider, N. T., Wagenmaker, E. R., Jayasundera, V. B. and Omary, M. B. (2012). Oxidative stress, Nrf2 and keratin up-regulation associate with Mallory-Denk body formation in mouse erythropoietic protoporphyria. *Hepatology* **56**, 322-331.

Snider, N. T., Weerasinghe, S. V., Singla, A., Leonard, J. M., Hanada, S., Andrews, P. C., Lok, A. S. and Omary, M. B. (2011). Energy determinants GAPDH and NDPK act as genetic modifiers for hepatocyte inclusion formation. *J. Cell Biol.* **195**, 217-229.

Strnad, P. and Omary, M. B. (2009). Transglutaminase cross-links Sp1-mediated transcription to ethanol-induced liver injury. *Gastroenterology* **136**, 1502-1505.

Strnad, P., Harada, M., Siegel, M., Terkeltaub, R. A., Graham, R. M., Khosla, C. and Omary, M. B. (2007). Transglutaminase 2 regulates mallory body inclusion formation and injury-associated liver enlargement. *Gastroenterology* **132**, 1515-1526.

Sugawara, M., Kato, K., Komatsu, M., Wada, C., Kawamura, K., Shindo, P. S., Yoshioka, P. N., Tanaka, K., Watanabe, S. and Toyoshima, I. (2000). A novel de novo mutation in the desmin gene causes desmin myopathy with toxic aggregates. *Neurology* **55**, 986-990.

Tatsukawa, H., Fukaya, Y., Frampton, G., Martinez-Fuentes, A., Suzuki, K., Kuo, T. F., Nagatsuma, K., Shimokado, K., Okuno, M., Wu, J. et al. (2009). Role of transglutaminase 2 in liver injury via cross-linking and silencing of transcription factor Sp1. *Gastroenterology* **136**, 1783-1795.e10.

Tutois, S., Montagutelli, X., Da Silva, V., Jouault, H., Rouyer-Fessard, P., Leroy-Viard, K., Guénet, J. L., Nordmann, Y., Beuzard, Y. and Deybach, J. C. (1991). Erythropoietic protoporphyria in the house mouse. A recessive inherited ferrochelatase deficiency with anemia, photosensitivity, and liver disease. *J. Clin. Invest.* **88**, 1730-1736.

Williams, M., Van der Zee, J. and Van Steveninck, J. (1992). Toxic dark effects of protoporphyrin on the cytochrome P-450 system in rat liver microsomes. *Biochem. J.* **288**, 155-159.

Wilson, K. L. and Foisner, R. (2010). Lamin-binding proteins. *Cold Spring Harb. Perspect. Biol.* **2**, a000554.

Worman, H. J. (2012). Nuclear lamins and laminopathies. *J. Pathol.* **226**, 316-325.

Zatloukal, K., Denk, H., Spurej, G. and Hutter, H. (1992). Modulation of protein composition of nuclear lamina. Reduction of lamins B1 and B2 in livers of griseofulvin-treated mice. *Lab. Invest.* **66**, 589-597.

Zatloukal, K., French, S. W., Stumptner, C., Strnad, P., Harada, M., Toivola, D. M., Cadrin, M. and Omary, M. B. (2007). From Mallory to Mallory-Denk bodies: what, how and why? *Exp. Cell Res.* **313**, 2033-2049.